IEEE Access
Multidisciplinary : Rapid Review : Open Access Journal

Received April 17, 2017, accepted May 21, 2017, date of publication May 26, 2017, date of current version June 27, 2017.

Digital Object Identifier 10.1109/ACCESS.2017.2708658

Physical Human–Robot Interaction (pHRI) in 6 DOF With Asymmetric Cooperation

BRYAN WHITSELL, (Member, IEEE), AND PANAGIOTIS ARTEMIADIS, (Senior Member, IEEE)
School of Engineering for Matter, Transport and Energy, Arizona State University, Tempe, AZ 85287 USA

Corresponding author: Panagiotis Artemiadis (panagiotis.artemiadis@asu.edu)

ABSTRACT Human–robot interaction is a growing area of research as robotic applications expand into unstructured environments. However, much of the current research has focused on tasks involving limited degrees of freedom (DOF), while not allowing the human the ability to choose the DOF on which they wish to focus. In this paper, a controller that allows human–robot cooperation in six-DOF Cartesian space is presented, which allows the human to direct their focus as they desire. The developed scheme was tested using a virtual reality system while maintaining physical interaction with the robot. Overall, the subjects were 100% successful in completion of the tasks and were able to exchange leader/follower roles with the robot bidirectionally. In addition, a reinforcement learning algorithm was shown to decrease the estimated mechanical power applied by the human to exchange roles. The latter proves the efficiency of the proposed scheme and makes it a strong candidate for applications that involve sophisticated human–robot interaction in collaborative tasks found in a plethora of cases, e.g., industry, manufacturing, semi-autonomous driving, and so on.

INDEX TERMS pHRI, physical human-robot interaction, cooperation, reinforcement learning, virtual reality, augmented reality.

I. INTRODUCTION

The physical interaction of a human with a robotic system is an essential part of an increasing number of robotic applications. Robotic systems are being successfully used in the rehabilitation of humans [1], in exoskeletons to improve human ability [2], [3], and as an aid to workers [4]. Additionally, researchers have been investigating the use of machine learning algorithms to improve this interaction as in [5]–[7].

One important type of interaction is cooperation. For our purposes, we define human-robot cooperation as a human and robot physically interacting to achieve an overall goal. When a human and robot are cooperating together, there typically is a role assignment for the human and robot. One of the most common methods is to permanently assign the role of the robot as the follower of the human. Kosuge *et al.* [8] proposed a method for using impedance control of multiple robots to aid a human moving an object and conducted an experiment with motion along one degree of freedom (DOF). Duchaine and Gosselin [9] developed a controller using variable impedance for human-robot interaction. The robotic system determines if the human's intent is to accelerate or decelerate. It then either decreases or increases damping (impedance to velocity) to aid the human. This system always acts a follower to the human and was tested in a two DOF maze task and a three DOF pick and place task. Corteville *et al.* [10] examined a human-robot cooperation controller. The robotic system only acts as a follower of the human in a one degree of freedom task. They created an estimator to determine the desired motion assuming a bell-shaped velocity profile. Bussy *et al.* [11] examined human-robot cooperation in a three DOF planar task. The robotic system predicts the motion of the human and actively follows by aiding in that motion. Tsumugiwa *et al.* [12] created a variable impedance controller for human-robot interaction. They tested this controller on a three DOF task and found that impedance of the robot aided the human in placing the object accurately. Passenberg *et al.* [13] used a two DOF haptic device to interact with a computer to simulate a human-robot interaction and investigated optimization of the assistance provided by the robot to the human. This research has improved the methods available for a robotic system to follow a human.

The ability of a robotic system to follow the lead of the human is important. However, many compelling applications of human-robot interaction are where the robotic system could provide elements that the human cannot or would prefer not to provide. For these types of applications, some method of exchanging roles between the human and the robot would be essential. Role exchange between humans and robotic systems has been examined in two main ways, the study of human-human interaction and human-robot interaction.

The goal of human-human interaction research is to extract useful concepts for later application in human-robot interaction. This has the potential of discovering ways for the robotic system to naturally interact with the human. Groten *et al.* [14] created a measurement of dominance between two humans interacting through a haptic one DOF knob. They showed that humans had a preference for a dominance differential when working together as opposed to mutually shared control. Additionally, there were differences in individual subject preferences to being more or less dominant. Madan *et al.* [15] investigated human-human cooperation in a planar three DOF task. The humans individually interacted with a haptic device and watched a separate computer display of the task. They were also presented with goals of the task and in some trials these goals conflicted. After the testing, they categorized the interaction of the two humans as harmonious, conflicting, and passive agreement. They were able to classify these states correctly in 81% of the time, using a support vector machine. Stefanov *et al.* [16] created two role categories in human-human interaction. One is execution and the other is conductor. They performed a one DOF experiment where each subject interacted with a haptic interface. They were then able to identify these roles through haptic data from the human-human experiment. Groten *et al.* [17] examined decision making in a human-human one DOF experiment. The subjects interacted with a one DOF haptic device and looked at a monitor for visual feedback. This was tested with and without haptic feedback and they found that haptic feedback improved performance.

Reed and Peshkin [18] also investigated human-human interaction. In a one DOF experiment, they found that the humans would specialize in different elements of the task. This specialization allowed for increased performance of the task. This is an important concept and it would be beneficial for human-robot systems to accommodate specialization within the task.

Researchers have also investigated this field by examining human-robot (or human-computer) interaction directly. This can help determine the unique issues that adding a robotic system can cause. Reed and Peshkin [18] found that humans rated the performance of a partner differently when they thought it was a human compared to when they thought it was a robot. Parker and Croft [19] examined a human-robot cooperative carry task of a long object. The task was a vertical lift with leveling, a two DOF task, they found that there were significant variations based on the speed of the task and differences between subjects. Oguz *et al.* [20] examined using a haptic device to control a two DOF virtual game with role exchange between the human and computer. Wojtara *et al.* [21] created a prototype robotic system for placing a thin, flat object on a surface. The robotic system only has a general location of the target position and the human interacts with the impedance of the robot to adjust the final position. Lawitzky *et al.* [22] utilized a two DOF haptic device to investigate an effort sharing paradigm. Balanced effort, minimum robot effort, and maximum robot effort behavior was analyzed.

Evrard and Kheddar [23] created a homotopy switching model that essentially created a continuous function of varying levels of leader roles. They tested this on a haptic device with two DOF virtual lifting task. One element from this experiment is that in numerous trials the computer was acting as the leader of the task, however the human subject believed they were the leader of the task. This suggest the need for more distinctive role exchanges and potentially relates to the preference in human-human dyads for disparity in dominance as noted above in Groten *et al.* [14].

Kucukyilmaz *et al.* [24] used a haptic device for a human-computer two DOF virtual task. They applied three conditions; one where there was equal control by the human and computer, one where there was a role exchange, and one where there was a role exchange with additional vibrational and visual cues regarding role allocation. They found that the role exchange method enhanced performance over the equal control method. However, the method with additional cues degraded performance.

One element that is often utilized in both human-human and human-robot research is the utilization of machine learning, as in Wang *et al.* [25] and Madan *et al.* [15]. This is done as a way of potentially improving the control of a robotic system and the interaction with the human.

A. MOTIVATION

From examining the prior research, there are several limitations to be considered. The first is that much of the prior research focusses on using limited numbers of degrees of freedom. One of the main goals of the field is for humans and robotic systems to be able to cooperate in an unstructured everyday environment De Santis *et al.* [26]. If robotic systems are going to be utilized in these types of environments, then they need the DOF and the control methods to do so. This means that studies involving full six DOF cooperation need to be pursued. This tests both the complexity of the robotic control as well as the ability for the human to interact along these various axes simultaneously.

Second, a number of researches have utilized haptic interfaces to simulate physical interaction. While this has led to meaningful research, to continue to move the field forward, research needs to be done that utilizes the types and scale of physical interaction with a robotic system that future unstructured applications will demand. Many of the haptic devices would be excellent choices for telerobotic applications but they offer very different physical interaction dynamics than physical interaction with robotics. Additionally, in an unstructured environment, the human may choose to grip the object of interest in a variety of different ways during the task and even switch between manual and bimanual manipulation.

Many haptic devices significantly limit or preclude the human from performing these types of variations.

Robotic systems need to be able to adapt. There are significant differences between humans, but also there is a need to be able to adapt to the task. Humans are limited in the numbers of things they can focus on. Robotic systems need to be able to adapt to the human both with regard to individual differences and to what part of the task that the human is currently focusing on (or specializing in as in Reed and Peshkin [18]). Allowing the human to vary the number of DOF to focus on creates a cooperation with the robotic system that is asymmetric. We define asymmetric cooperation as cooperation where the ratio of leader roles between the human and robotic system can vary. As an example, the robotic system could be a leader in four DOF and this would allow the human to only need to focus on leading two DOF.

Finally, robotic systems that operate in an unstructured environment may have incomplete or incorrect information and experiments need to reflect this.

To meet these challenges, this research will:

1) Utilize 6 DOF human-robot cooperation while maintaining realistic physical human robot interaction.
2) Allow the human to choose what to focus on by using a controller that allows asymmetric cooperation.
3) Test in an environment that includes mistakes made by the robotic system.
4) Improve this cooperation and adaptability by utilizing machine learning.

The rest of the paper is organized as follows. Section II presents the development of the virtual reality (VR) physical human robot interaction system (pHRI). Section III presents the controller of the robotic system. The experimental methods are presented in Section IV. The results of the experiments are presented in Section V, while Section VI concludes the paper.

II. DEVELOPMENT OF VR pHRI SYSTEM

One of the main goals of our research was to examine human-robot cooperation in 6 DOF Cartesian space. In order to accomplish this, we needed a robotic system that was controllable in this space. We also needed to create a necessity for the human and robot to interact in the full 6 DOF space. The former requirement was satisfied by using a KUKA LBR iiwa robotic arm that has 7 DOF, the details of which will be discussed later. The latter requirement however created some possible concern. To create tasks that require cooperation in 6 DOF, there needed to be restrictions along these axis.

Our initial concept was to create a physical obstacle or restriction that the human and robot have to negotiate during the cooperative task. However, building physical restrictions has the potential to place the human at greater risk of injury and creating a greater risk of damage to the robotic system. To deal with this risk, we choose to create virtual restrictions in a virtual reality system while preserving the real physical interaction of the human and robotic system. As mentioned previously, maintaining the physical interaction between the human and robot was an essential element to this research.

One of the main concepts of this system was to display an object virtually to the human that also corresponds to a real object that was connected to the end of the robot and that the subject physically interacts with. This system also displays virtual restrictions to the user so they can understand the desired task motion. For this experiment, a virtual wall was displayed to the user with a hole in the wall. This hole in the wall varied in location and orientation matching to a particular 6 DOF solution that the user and the robot must cooperate to achieve.

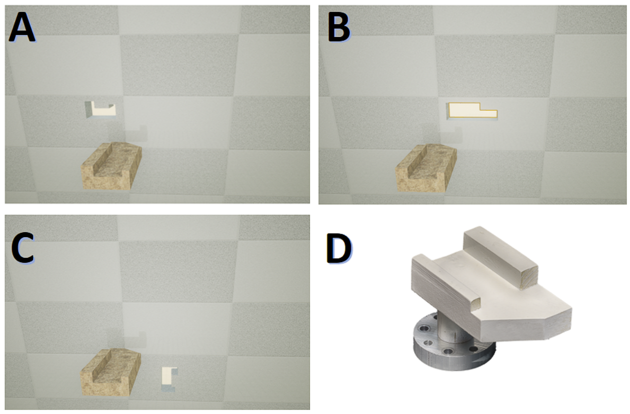

FIGURE 1. Virtual Wall and Jointly manipulated Object- A, B, and C are the virtual holes for position 1, 2, and 3 respectively. D was the jointly manipulated object attached to the end of the robotic arm.

A visual system needed to display to the subject the virtual world. For this, Unreal Engine 4 was chosen for its ability to display objects in three-dimensional space, compatibility with various VR headsets, and a simple licensing agreement. A virtual world was created in this system. This world had a virtual wall with a hole displayed that would be used in the experiment as well as the virtual representation of the jointly manipulated object as shown in Fig. 1. There were three different possible holes. Only one of the holes would be displayed at a time during the experiment.

For each trial, the hole for that trial was displayed. To coordinate the motion of the block in the virtual world with the real world, a network connection was created between the robotic control system and the computer system running the visualization code. This network connection allowed the computer that ran the robotic control software to send position and orientation data to the visualization system. For this experiment, the physical feedback of running into the virtual wall was unnecessary since the purpose of the experiment was to examine the interaction of the robot and human prior to arriving at the goal location, although this would be possible for future experiments.

To display the virtual reality to the human, an Oculus Rift was used. This was the current commercially available version (CV1). It has a separate position sensor that determines the absolute position of the headset with respect to the sensor. This was useful because it takes into account both rotation of the headset as well as translation.

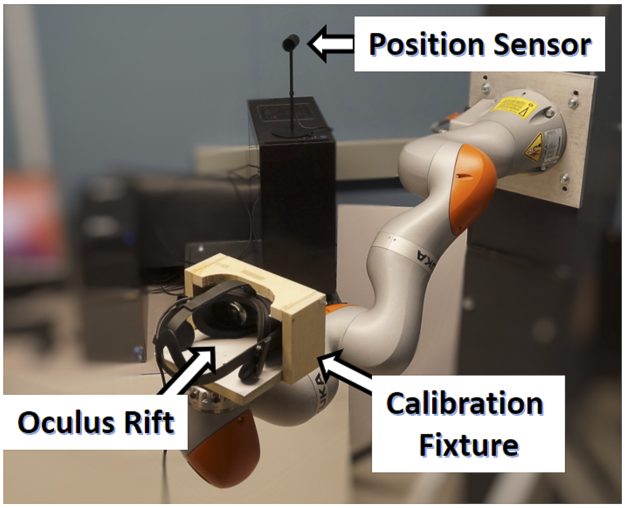

FIGURE 2. Virtual and Real World Alignment.

One difficulty encountered was aligning the virtual and real worlds together, and an initialization procedure was created. Prior to each session with the robot, the robot was placed in a specific position and a fixture was attached as seen in Fig. 2. This fixture was designed to hold the headset in a specific location and orientation. The VR headset position was then reset using an internal menu in the system. This zeroed position corresponds to the initial camera position in the virtual reality software, Unreal Engine 4. The experimenter then verified that the virtual system was aligned with the real world. Although difficult to create an exact measurement, the discrepancy of the object in the virtual world with the object in the real world appeared to be less than 5 mm. Additionally, this system maintains the accuracy throughout the experiment. Most of the subjects (4 out of 6) spontaneously made positive comments on the accuracy with which the virtual and real world matched. No negative comments were made by the subjects.

III. ROBOTIC CONTROL METHODS

For this experiment, a 7 DOF robotic arm was used (KUKA LBR iiwa). This robotic system utilizes KUKA's SunriseOS software on the robotic controller. This software allows for a number of possible control methods. For interaction between humans and robotic systems, we desired to utilize impedance control. By using impedance control we are able to give the robotic arm a level of compliance to external interaction. Impedance control uses displacement as the input to the system with force and torque as the output. The tasks that the robotic system and the human will be engaged in are best described in Cartesian space. For this reason, we desired to control the robot also in Cartesian impedance control. Mechanical impedance is described by equations (1) - (4).

$$\overline{\mathbf{F}} = \begin{bmatrix} F_x \\ F_y \\ F_z \end{bmatrix} = M\ddot{x} - B_t\dot{x} - K_t x \tag{1}$$

$$\overline{\mathbf{T}} = \begin{bmatrix} T_x \\ T_y \\ T_z \end{bmatrix} = J\ddot{\theta} - B_r\dot{\theta} - K_r\theta \tag{2}$$

$$K_t = \begin{bmatrix} k_{tx} & 0 & 0 \\ 0 & k_{ty} & 0 \\ 0 & 0 & k_{tz} \end{bmatrix} \quad x = \begin{bmatrix} x_p - x_e \\ y_p - y_e \\ z_p - z_e \end{bmatrix} \tag{3}$$

$$K_r = \begin{bmatrix} k_{rx} & 0 & 0 \\ 0 & k_{ry} & 0 \\ 0 & 0 & k_{rz} \end{bmatrix} \quad \theta = \begin{bmatrix} \alpha_p - \alpha_e \\ \beta_p - \beta_e \\ \gamma_p - \gamma_e \end{bmatrix} \tag{4}$$

where $\overline{\mathbf{F}}$ was the force vector along the x, y, and z directions. $\overline{\mathbf{T}}$ was the torque vector generated about the x, y, and z axis. The mass matrix, M,and the rotational inertia matrix, J, are computed by the robotic system during the experiment. B_t and B_r are the damping coefficients matrices for translation and rotation and are effected by the damping ratio for the experiment. K_t and K_r are the stiffness matrices for translation and rotation respectively. The dampening ratio was set at 1 and remains constant throughout the experiment. The stiffness was set at $k_{tx} = k_{ty} = k_{tz} = 600N/m$ and $k_{rx} = k_{ry} = k_{rz} = 15Nm/rad$ when the robotic system was acting as the leader of that DOF and $k_{tx} = k_{ty} = k_{tz} = 300N/m$ and $k_{rx} = k_{ry} = k_{rz} = 15Nm/rad$ when it was acting as the follower. The current translational position was represented by (x_p, y_p, z_p) and the current orientation was $(\alpha_p, \beta_p, \gamma_p)$. The equilibrium position was represented by (x_e, y_e, z_e) and $(\alpha_e, \beta_e, \gamma_e)$ for translation and rotation respectively. Additionally, α, β, and γ are roll, pitch, and yaw angles respectively. For an in depth look at impedance control of robotics, see [27].

The KUKA LBR iiwa has more than one method for creating Cartesian impedance control. KUKA's Direct Servo control system was used. This allows for the equilibrium point in impedance control to be specified in Cartesian space as well as modifying the stiffness values, features that were not supported by the other methods. The timing of the command cycle of the robot was typically at 5ms per cycle.

A. HUMAN-ROBOT COOPERATION CONTROL

For our cooperative control system, we are using three different states for each DOF. These states are robot leading, robot following, and a transitional state between these leader/follower states.

Our research creates the ability for the human and the robot to cooperate asymmetrically. This means that the human can be the leader of as many or as few of the DOF that he/she desire to be in order to achieve the overall goal. The control diagram can be seen in Fig. 3, which is explained below.

1) DESCRIPTION OF HUMAN-ROBOT CONTROL DIAGRAM

Leader Trajectory is the trajectory when the robotic system was acting as the leader for a particular DOF. This trajectory

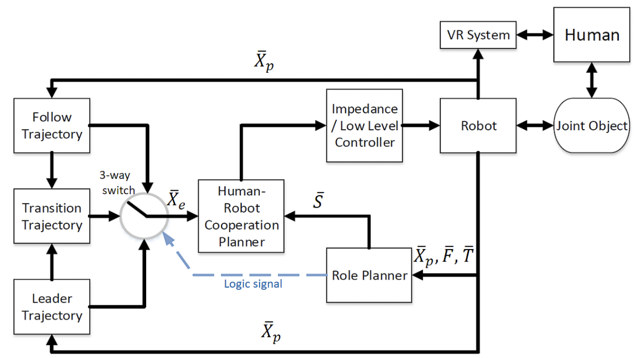

FIGURE 3. **Human-Robot Control Diagram.**

was generated using eq. (5) which is a fifth order spline with the form given in [28].

$$m_{tr} = m_s + (m_e - m_s)\left(10(\tau)^3 - 15(\tau)^4 + 6(\tau)^5\right) \quad (5)$$

The starting value was m_s and m_e was the ending value. The next value in the trajectory was m_{tr}. This equation relies on τ to progress the trajectory toward the goal. To do this, two methods were used. The first was time and τ was a ratio of the elapsed time divided by 6 seconds. This was used only for the DOF moving toward the wall (x-axis). For the other values of τ, we used a ratio for how far the object had moved from its starting position toward the wall along the x-axis. Additionally, we also stipulated that if the object was moved closer to the end goal than the trajectory equilibrium point, then that point was used. This allowed the human to positively influence the motion towards the goal without necessarily taking over as leader of that axis. When the robot was the leader of a translational DOF, the stiffness value for that axis was set to 600 N/m, while for a rotational axis it was set to 15 Nm/rad.

Follower Trajectory is the trajectory when the robot is following the robotic system. For this experiment, we used a passive follower, where m_{tr} was equal to the last measured position. This makes the robotic system compliant along that axis. However, from some pilot studies, it was felt that increasing the damping may be useful in the follow mode in the rotational axis. To achieve this the stiffness value for the impedance control for rotation was maintained at 15 Nm/rad. For the translational case, it was reduced to 300 N/m. Because the equilibrium point was reset at each command cycle to the last measured position, the effect of the stiffness was seen on the amount of motion that has occurred during the previous command cycle. This has the effect of dampening even though it was being implemented using stiffness.

The *Transition Trajectory* was needed to transition the robot to either the follower or leader mode. This was done over 125 command cycles of the robot (0.6 seconds). This utilized a fifth order spline similar to equations (5). The difference was the initial state was the trajectory of the current role and the final state was the trajectory of the new role. The value of τ is the fraction of the current number of cycles of transition divided by 125 cycles. After 125 cycles the transition was complete and the next command cycle will be the new role (leader or follower).

The *Role planner* determines if the robotic system needs to switch from its current role (leader or follower) to a different role. This was substantially different for the threshold method compared to the machine learning method and will be discussed in detail in the role determination section.

The *Human Robot Cooperation Planner* takes the new equilibrium point and the stiffness value for each DOF. It aggregates the 6 DOF into a single impedance control command and sends this to the Impedance/Low Level Controller.

The *Impedance/Low Level Controller* system takes the impedance control command and creates the low level control command to control the robotic system.

2) ROLE DETERMINATION WHEN ROBOT IS LEADER

For determining if the human wanted to take over as leader of a DOF from the robotic system, two methods were evaluated. The first was a threshold method based on the force (or torque) applied along individual DOF. The second was a reinforcement learning algorithm that used force and torque as an input to predict the value of future rewards for either staying as the leader or switching to the follower.

For the threshold method, a value of force (or torque in the rotational DOF) was used to determine if the human wants to take over as leader of the DOF being evaluated. This was done by comparing the absolute value of the current force (or torque) with a threshold value. A switch of a leader was initiated if this value was larger than the threshold. This is described by the equations (6)-(10). The threshold values that were chosen were determined based on previous experiments as well as an initial pilot study that was done prior to this experiment.

For the purposes of clarity and compactness of equations involving different types of DOF, we defined three sets a, b, and c as in equation (11). a is the set of translational DOF. b is the set of rotational DOF. c is all DOF, or $a \cup b$. The subscripts a, b, and c are used to denote that a variable applies to all members of that set. In summation, if the variable has an a subscript then it is valid for all translational DOF. For a b subscript, it is valid for all rotational DOF. For a c subscript, it is valid for all DOF. Additionally, a variable with a subset in parentheses, such as $x_{(n)}$ means that it is the n^{th} sample of that variable in time.

$$\bar{\mathbf{S}} = \left[S_x \; S_y \; S_z \; S_\alpha \; S_\beta \; S_\gamma\right] \quad (6)$$

$$\bar{\mathbf{R}} = \left[R_x \; R_y \; R_z \; R_\alpha \; R_\beta \; R_\gamma\right] \quad (7)$$

$$R_c = \begin{cases} 1, & \text{robot leads DOF} \\ 0, & \text{otherwise} \end{cases} \quad (8)$$

$$S_a = \begin{cases} 1, & \text{if } F_a > C_1 \text{ and } R_a = 1 \\ 0, & \text{otherwise} \end{cases} \quad (9)$$

$$S_b = \begin{cases} 1, & \text{if } T_b > C_2 \text{ and } R_b = 1 \\ 0, & \text{otherwise} \end{cases} \tag{10}$$

$$a \in \{x, y, z\} \quad b \in \{\alpha, \beta, \gamma\} \; c \in \{x, y, z, \alpha, \beta, \gamma\} \tag{11}$$

where F_a was the force applied to the joint object by the human and T_b was the torque applied. These values are estimated by the robotic system using the measured joint torques values for the 7 joints on the robotic system. $C_1 = 12N$ and $C_2 = 2Nm$. $S_c = 1$ was the value that indicates that a switch is to take place along the particular DOF. $R_c = 1$ indicates that the robot was leading that DOF.

The other method evaluated was a reinforcement learning algorithm. Reinforcement learning is one type of unsupervised learning algorithms. This was chosen because it was desired for the system to be able to learn and improve its interaction with a human without requiring the additional input needed for a supervised learning algorithm to function. In reinforcement learning the system makes choices based on expected rewards or the expected value of the summation of the rewards.

One method for determine what the rewards would be for a decision is to use a predetermined model that equates the inputs to rewards. This approach can be very useful for a number of applications for which a reliable model can be determined. These types of algorithms very closely resemble optimal control and the optimization of rewards. The predetermined model however has two assumptions inherent to it. The first is that an accurate model can be predetermined and that the system does not change with time. For our application, we know of no predetermined model that can accurately predict how a human will generally react and interact with a robotic system. Additionally, humans vary between each other and adapt their behaviors.

To address the above consideration, a different technique for reinforcement learning was used. This was where the system learns to predict what the future rewards of an action will be based on past rewards gained from this action. This allows the system to learn and adapt to the interaction as well as change over time as conditions change. The difficulty that arises from a system that uses this type of method is the initial operation. The initial operation for a robotic system interacting with a human needs to perform in a safe and predictable manner. We accomplished this by initially giving the system data to make decisions based off of but replacing the data with experientially determined data once that it was available.

In reinforcement learning, the algorithm used to determine the values of the rewards profoundly impacts the way the system acts. At a conceptual level, we had two main goals. First, we wanted the system to not require the human to apply a large amount of physical effort to take over as leader of a DOF. Secondly, we desired to penalize the system for giving the human the lead of a DOF when the human was not trying to become the leader. These were the overall concepts behind our implementation. It is important to acknowledge that the specific implementation of these concepts did not perfectly reflect the conceptual idea and was based on estimated values, but it is useful to understand the underlying goals of the implementation.

For the first goal of this strategy, we want to minimize the effort that the human applies to the system in order to take the lead of a degree of freedom. To turn this conceptual idea into practice we settled on utilizing an estimate of the mechanical power applied by the human. This value is an estimate and is not without controversy. One can argue that it is difficult (or impossible) to precisely determine the power contributed by the human engaged in a joint action with a robot, since it also relies on the interaction from the robot. Additionally, we utilized the estimate of the force and torque applied by the human at the end effector. This was estimated by the system based off of the torque values measured at the joints of the robot. A more accurate assessment of the input could be created by utilizing extra components such as instrumented handles for the human to interact with. However, this would have created specific requirements and limitations on the use and application of the robotic system. While adding additional components and sensors to the experiment may provide data with less noise, it also detracts from the ability of this system to be utilized in an unstructured environment which was one of the main goals of this research.

As mentioned above, we utilized an estimate of the mechanical power input by the human. This was applied as a negative reward (penalty) for the system. This reward was tied to an input variable (applied force and torque of the human). The input and this reward are shifted in time so that the input of force (or toque) will be used to predict the future power that the human will apply to the system. This was evaluated separately along each individual DOF. Work is defined as a force applied over a distance as in equations (12). Power is the time rate of mechanical work.

$$W_a = \int |F_a| \, da \quad W_b = \int |T_b| \, db \tag{12}$$

$$P = \frac{dW}{dt} \tag{13}$$

To calculate the power input by the human we first utilize the estimated externally applied force and torque values from the KUKA robotic system. We combine this with the distance traveled to yield mechanical work, as described by equation (12). To calculate the average power over time equation (14) was used. i was the index of the data history for the previous trial. g was one less than the number of samples the average was calculated over.

$$P_c = \frac{\sum_{n=i}^{i+g} W_{c(n)}}{t_{(i+g)} - t_{(i)}} \tag{14}$$

P_c was the average power that begins at the current sample, i, and continues till $i + g$. This was calculated to determine the average power that will be expended by the human. If $S_{c(i)} = 0$ and remains 0 for 200 cycles, then $g = 199$. However, if it switches during these 200 cycles then g was equal to the last cycle before the switch. In essence, this calculates the average power applied by the human in the stay condition for either 200 cycles going forward or up until it switches. To calculate P_c for the switch condition, it begins at the sample that the switch began and $g = 199$.

To prevent the system from switching unnecessarily, an additional penalty (negative reward) was created. This penalty would be assessed if the velocity of the end effector was below a threshold immediately after the human was given the lead of that DOF. The assumption was that the human was trying to lead the robot to the correct location when they intend to take over as leader of a DOF. The result of this would be that the velocity along this DOF would not be zero or near zero immediately after switching leadership to the human. Because there can be some motion due to noise in measurement or other unintentional motions from the human, a threshold value was used to determine if the human intended the robot to give them the lead along a DOF. This is described in equations (15) and (16).

$$Q_a = \begin{cases} 1, & |q_{(j+h)} - q_{(j+h-1)}| < C_3 \\ 0, & \text{otherwise} \end{cases} \tag{15}$$

$$Q_b = \begin{cases} 1, & |u_{(j+h)} - u_{(j+h-1)}| < C_4 \\ 0, & \text{otherwise} \end{cases} \tag{16}$$

where q was the translational position at the index specified. u was the rotational position at the index specified. j was index at start of switch of roles. h was 126 cycles. C_3 =1.0 mm $C_4 = 0.2\ mrad$. Q was the penalty for the DOF.

$$V_t = -P_c \tag{17}$$

$$V_w = -P_c - Q_c \tag{18}$$

where V_t was the value of the rewards for staying. V_w was the value of the rewards for switching.

For our reinforcement algorithm, we desired that the learned rewards for a given force would be an average reward for an applied force. To do this we choose to discretize the force and torque inputs into bins. The process of determining the correct bin is described by equations (19) and (20). The system averages the rewards scored for a force input within its bin. This is described in equations (21) and (22). This was a simple way of averaging out noisy values. This average will be used for the algorithm to predict the value of the rewards it will receive by staying the leader of a DOF or switching to the human as the leader of that DOF.

$$N_b(T_b) = \begin{cases} 1, & |T_b| < C_4 \\ \lfloor (|T_b| - C_4) \times 4 \rfloor, & \text{otherwise} \\ 10, & |T_b| \geq C_5 \end{cases} \tag{19}$$

$$N_a(F_a) = \begin{cases} 1, & \text{if } |F_a| < C_6 \\ \lfloor |F_a| \rfloor - C_6, & \text{otherwise} \\ 10, & \text{if } |F_a| \geq C_7 \end{cases} \tag{20}$$

where $\lfloor x \rfloor = max\{n \in \mathbb{Z} | n \leq x\}$ and N_c was the bin number for the force or torque applied to each of the 6 DOF. C_4 = 1.0 Nm and C_5 = 3.0 Nm. C_6 = 7.0 N and C_7 = 15.0 N. These values were chosen based on prior studies and pilot testing.

$$A1_c(N_c) = \frac{\sum_{n=1}^{l_1} V_{t(n)}}{l_1} \tag{21}$$

$$A2_c(N_c) = \frac{\sum_{n=1}^{l_2} V_{w(n)}}{l_2} \tag{22}$$

where $A1_c$ was average learned rewards for staying for that bin and DOF. l_1 was the total number of values that have been averaged for that bin and DOF. $A2_c$ was average learned rewards for switching for that bin and DOF. l_2 was the total number of values that have been averaged for that bin and DOF.

For reinforcement learning to work, it needs to explore to determine other possible solutions. When the system is exploring, it is choosing to make a decision that is less optimal based on what it already has learned. This is to help the system learn if a different value results in a better reward. To accomplish this a random number was generated with an even distribution from 0 to 1. As described in equations (23) - (25)

$$r_n \sim U([0\ 1]) \tag{23}$$

$$E = \begin{cases} -1, & r_n < 0.25 \\ 0, & 0.25 \leq r_n \leq 0.75 \\ 1, & r_n > 0.75 \end{cases} \tag{24}$$

$$A2_c(N_c + E) > A1_c(N_c) \wedge R_c = 1 \rightarrow S_c = 1 \tag{25}$$

were r_n was a random number. E was the exploration value. N_c was the bin value for a DOF. The comparison was then made between staying and switching as in equation (25) and S_c was set to one if the switch occurs if not it remains 0. This was not evaluated if the system has not completed the transition from a previous switch. However, this was evaluated across all 6 DOF each command cycle so that the system can switch leader follower roles across multiple DOF simultaneously.

At the beginning of each session, the machine learning algorithm was initialized and has no information from previous sessions. For this experiment and in applications, the robotic system needs to be able to cooperate with the human from the beginning. The $A1_c$ and $A2_c$ are initialized according to equations (26) and (27).

$$N_c \leq 4 \rightarrow (A1_c(N_c) = 0 \wedge A2_c(N_c) = -1) \tag{26}$$

$$N_c > 4 \rightarrow (A1_c(N_c) = -1 \wedge A2_c(N_c) = 0) \tag{27}$$

The result of this was that at the start of the session the system behaves as if there was a force or torque threshold at $N_c = 5$.

3) ROLE DETERMINATION WHEN ROBOT IS FOLLOWER

For this experiment, the robot needs the ability to change roles from leading a task to following a task and also the reverse of this. This was needed to allow the human the ability to focus on fewer DOF if desired.

To determine if the human wants the robot to take over an axis, we assume that the human was not currently using that axis and utilize the history of the motion along that axis as well as the history of the force (or torque in the rotational case) along the axis. To create an efficient method that would be robust against measurement noise, we used the 200-sample moving average of these values and compare these values against a threshold, as described in equations (28)-(32).

$$h_a = \frac{1}{C_7} \sum_{n=i-C_7}^{i} F_{a(n)} \tag{28}$$

$$h_b = \frac{1}{C_7} \sum_{n=i-C_7}^{i} T_{b(n)} \tag{29}$$

$$j_c = \frac{1}{C_7} \sum_{n=i-C_7}^{i} w_{c(n)} - w_{c(n-1)} \tag{30}$$

where h_a was moving average of the force applied along a DOF $\in a$. C_7 was 200 cycles. h_b was the moving average of the torque applied along a DOF $\in b$. j_c was the moving average of the change in position along a DOF $\in c$. $w_{c(n)}$ was the position at cycle n along a DOF $\in c$.

$$|h_a| > C_8 \wedge |j_c| > C_9 \wedge R_a = 0 \rightarrow S_a = 1 \tag{31}$$

$$|h_b| > C_{10} \wedge |j_c| > C_{11} \wedge R_b = 0 \rightarrow S_b = 1 \tag{32}$$

where $C_8 = 0.3N$ $C_9 = 1.0\ mm/cycle$ $C_{10} = 3.0\ N/mm$ $C_{11} = 0.02\ mrad/sec$

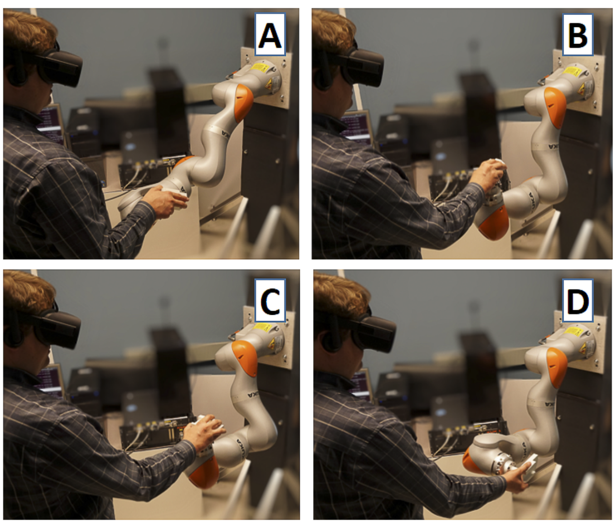

FIGURE 4. **Human Robot Interaction-A was initial position. B, C, and D are poses 1, 2, and 3 respectively.**

IV. EXPERIMENTAL METHODS

A. PHYSICAL AND VIRTUAL EXPERIMENT SETUP

1) PHYSICAL SETUP AND VIRTUAL SETUP

The initial pose and the final poses for the three different holes can be seen in Fig. 4. The start pose for all trials was (0 mm, 0 mm, 0 mm, 35°, −30°, 35°). The final poses are (165 mm, 75 mm, 50mm, 0°, 0°, 0°), (165 mm, −75 mm, 50mm, 0°, 0°, 90°), and (165 mm, −75 mm, −110mm, 90°, 0°, 0°) for pose one, two, and three respectively. The three different hole locations and orientations can be seen in Fig. 1. Since the robot is kinematically redundant, the exact configuration of the arm for each of those locations can vary keeping the final position of the joint object the same.

B. EXPERIMENT PROTOCOL

For this experiment, six subjects participated. Each subject performed five sessions, each session on a different day. The first session was a training session and utilized the threshold method for all subjects. This session was used as a way of decreasing the effect of the subject learning the task on the data. The subjects were not told that the first session was a training session and the data from that session was not analyzed. Other than that, the session was conducted the same as the remaining four sessions.

Each of the subjects performed two threshold and two machine learning sessions after the initial training session. The types of sessions alternated between threshold and machine learning. Three of the subjects started with the threshold control algorithm for their first session after the training session. The other three started with machine learning algorithm. The subjects were not informed which type of control scheme was being used during their session.

Each session was composed of 60 trials. Each of the three walls were used for 20 trials. In half of the trials, the robot would move have the correct goals. In the other half, the robot would have incorrect information as to the goal and would use one of the other two positions. Additionally, half of the experiments the subject started the trial being in control of three degrees of freedom of translation and the robot leading the three degrees of freedom of rotation. In the other half, these starting roles were reversed.

Each subject completed 240 trials (excluding training trials). Across all 6 subjects this totals to 1440 trials. The subjects were told that they were to cooperate with the robot to move the joint object to the correct position and orientation of the object which was the hole in the wall. The hole in the wall had an additional 5 mm removed around all edges to make it easier to put the object in the correct location. If the subject and robot moved the joint object to the correct location and orientation, it was judged a success. This was scored by the experimenter by verifying that the joint object was within the 5mm oversized hole in the virtual representation.

At the beginning of each trial, the subject acted as the leader of three degrees of freedom and the robot was the leader of the other three degrees of freedom. They were told at the beginning of each trial which degrees of freedom (translation or rotation) that they would start as the leader. They were then informed that after the start of the trial these roles can be exchanged with the robot. They were informed that sometimes the robot would go in the wrong direction or orientation and that they needed to correct the robot if it made a mistake. Additionally, they were told that the robot may take back over as leader of a DOF if it determined that the subject was not using it. Finally, the subjects were informed that they could change their grip on the object if they wanted to during the trial and that they were free to switch from using one hand to using both and it was completely up to them to decide. They were encouraged to cooperate with the robot in whatever way felt natural to them.

These experiments were conducted in accordance with ASU IRB # STUDY00004933.

V. RESULTS

A. COOPERATIVE RESULTS

Overall human-robot cooperation in 6 DOF cartesian space was successful. Out of the 1440 trials completed, the subjects and the robotic system were able to cooperate to place the block in the correct location and orientation 100 % of the time. In previous research [29], this was not always the case. If the human believed that the system was unresponsive, they would quit attempting to correct the robotic system when it was moving in the incorrect direction in this previous research. In this experiment, this was not the case and the human and robot were able to perform the cooperation successfully.

TABLE 1. Leader/follower role exchange.

Role Exchanges/trial	0	1	2	3	4	>4
Total	113	363	379	307	157	121
Percentage of Trials	7.8	25.2	26.3	21.3	10.9	8.4

The subjects and the robot were able to exchange roles of leader and follower of 6 DOF freely as can be seen in Table 1. The asymmetric cooperation concept, discussed earlier, allowed the human and the robot to cooperate in a way that customized the solution both to the unique problem and to the human. In Fig. 5, the leader status for the human and robot for a particular trial was plotted. This shows how the human was able to take over as the leader of roll and yaw axis to correct a mistake made by the robot and then the robot was able to take over as the leader of two of the translational axis. The robot maintains these axis in the position that it took them over in. This prevents the human from having to maintain the position of these axis while he/she completed the task.

The robot would take back leader of a DOF if the human was not moving it much and there were low forces over time. If the human then takes back leader of that axis, this may indicate an inefficiency when the human had to take back over as leader. Out of all six subjects, all four sessions, all 60 trials, and all six axes the robot took back leader of an axis 1702 times. Out of these 1702 times the human took back leader of that axis 76 times (4.4%). This means that 95.6% of time the robot was able to take over as leader and perform adequately. This shows the potential ability of this approach to lessen the humans need to lead an axis.

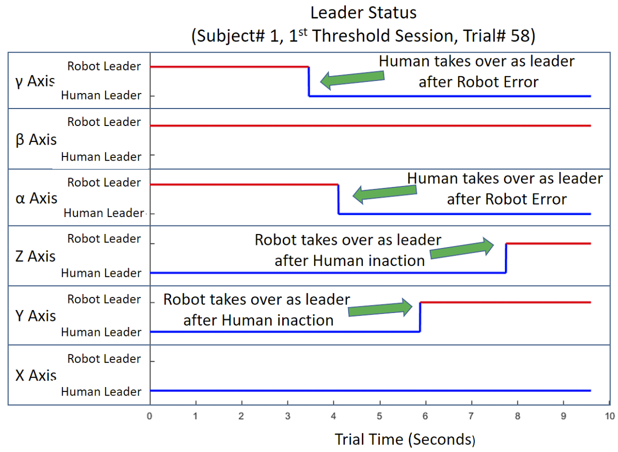

FIGURE 5. Leader Status - Human starts as leader of translational DOF and as follower of rotational DOF.

Allowing the human the ability to choose which degrees of freedom to lead resulted in some of the subjects behaving differently than anticipated. This can be seen in looking at the time that was taken to complete the tasks. The progress along the x axis was the main ways to control the pace of the experiment. When the robot was leading all three degrees of translation, the progress along the x-axis was based on time. The progress of all other axes are based on the distance away from the wall. Some of the subjects completed the trials at a significantly faster rate than the others. The main way that they were able to do this was by taking over as the leader of the x axis when it was not required. As can be seen in Fig. 6, the humans that completed the trials the fastest took over as the leader of the x axis at the highest rate. In Fig. 6, the subjects are ordered from fastest to slowest. This order also perfectly matches the order of percentage of trials where the human took over as leader of the x axis.

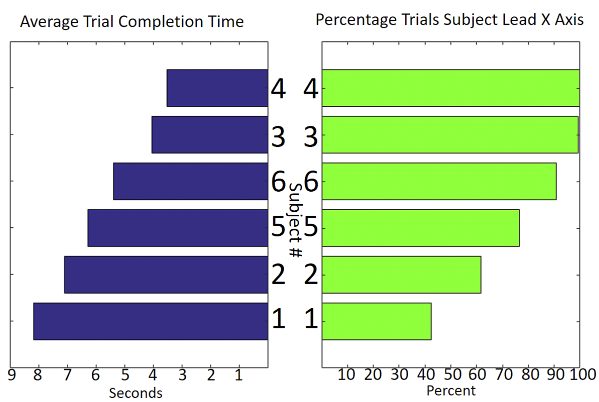

FIGURE 6. Completion Time and X axis Leader.

For subject 4 (fastest), out of the 60 trials where the robot was initially leading translation and will move to the correct location, subject 4 took over x axis 100% of the time. However, 55% of the time the subject only took over the lead of the x axis and the robot remained the leader of both y and z. Additionally, 36.7% of the time the subject took over only one additional translational axis. This means that 91.7% of the time the robot remained as the leader of at least one of the translational axis. This lessens the human's responsibility, while still allowing them to control the pace of the action.

However, this also produced interesting results at the slower completion time. In 50% of experiments the robot was going to the wrong location but the motion in x was correct. Subject 1 was able to correct the y and z axis while allowing the robot to continue being in control of the x axis in a number of trials. Thus, choosing to maintaining the pace of the trial at the speed that the robot was conducting it but correct for the robots positional error.

B. MACHINE LEARNING

In this experiment, the machine learning algorithm adapts the level at which the robot transfers leadership of a DOF to the human. In order to accomplish this, it uses force and torque values as a predictor of future power used as well as an additional penalty for switching unnecessarily. To examine the effects of the algorithm, power used to make a switch was performed. The power that the user applied to the robot to get the robot to switch to being the follower along a DOF was calculated. This was calculated as the average power over the 200 cycles prior to the switch (or fewer if the switch happened in less than 200 cycles from the start of the trial). These values were then averaged for all DOF for the threshold and the machine learning sessions separately. These values are then compared as the machine learning average as a percentage of the threshold values, as in Table 2. The overall average for every subject was lower power used to take over as leader for the machine learning sessions.

TABLE 2. Average power used to switch for ML trials (as % of the subjects average for threshold trials).

Subject #	1	2	3	4	5	6
Translation DOF %	37	82.5	83.3	70.4	74.9	64.1
Rotation DOF %	103.5	97.5	43.2	89.5	85.7	105.4
All DOF %	70.3	90	63.3	80	80.3	84.7

As noted earlier, force and torque values are put into bins for the machine learning algorithm. If the subject applies an increasing force to the system an effective threshold value can be determined by checking at which bin the robotic system would switch leadership of an axis. The final effective bin threshold was calculated for each session and difference between the two sessions that each of subjects did were then compared. Combining all subjects creates 36 comparisons. A zero means no difference for that axis between sessions. The histogram of these differences can be seen in Fig. 7. From the data, there appears to be some consistency (52% within $\pm$ one bin) but also some day to day variation of subjects. This suggests that both longer term adaptation with the ability of day to day variations could be beneficial.

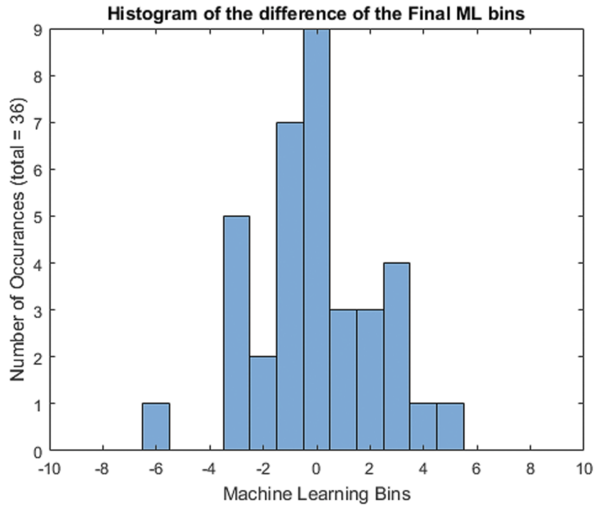

FIGURE 7. Histogram of consistency of ML.

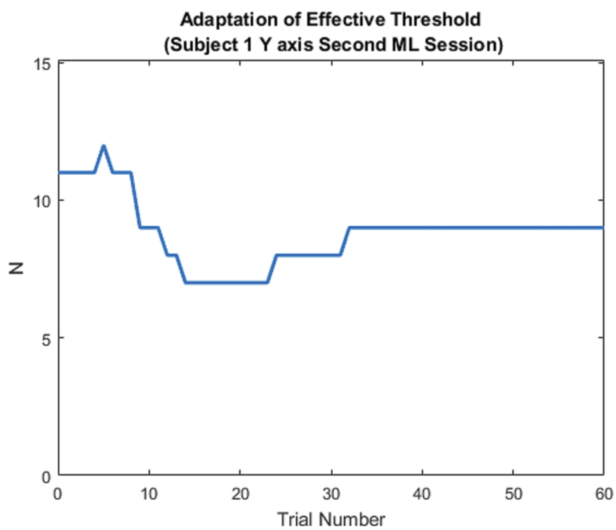

FIGURE 8. Adaptation of Effective Threshold.

The value of the effective bin changes over time as the system learns new information. A typical plot of this effective threshold for one subject and one axis can be seen in Fig. 8. The system adapts lower but then reacts to adapting too low and finds a stable value.

VI. CONCLUSIONS

There are several elements from this work that combine to contribute to the field of human-robot cooperation. Human-Robot cooperation was successfully performed in a 6 DOF environment by multiple subjects across multiple days. Asymmetric cooperation allowed the human to vary the numbers of DOF that he/she were the leader of during the trial. This interaction was improved using a reinforcement learning algorithm. Additionally, all of these elements were tested in an environment where the robotic system may make mistakes that the human needed to correct.

Overall, the VR pHRI system performed as expected during the testing. In order to expand its use for additional experiments, we have since added force interaction with virtual objects, a visual representation of the robotic arm, and an industrial factory virtual setting. For the purposes of this experiment we did not feel that these elements were needed. We did not use force interaction with virtual objects because our main focus was on testing the interaction between the human and robot prior to possibly interacting with the virtual wall. We also did not use a representation of the robotic arm or a more complex setting because we desired to limit the users focus to the jointly manipulated block and the 6 DOF motion. However, the additional complexities that these elements could add into the interaction are an additional interesting area of research. Overall, we felt that this type of system could be useful for a number of research experiments investigating human robot interaction, while preserving the complexities of actual physical interaction.

Some subjects' interaction with the system was innovative. In particularly, taking over as leader of the DOF that approaches the wall as a way of controlling and increasing the pace of the experiment. This unexpected adaptation by some of the subjects adds to the case for allowing humans the ability to choose which DOF they are leading and to have the robot lead the remaining DOF. From general observations during the experiment, subjects often broke down the task into stages and satisfied the position requirements sequentially. By allowing asymmetric cooperation, the subject was free to determine the order of meeting these requirements and the robotic system also was able to take back over as leader of a DOF and to maintain the location that the human had set.

Although not explicitly tested in this experiment, the response of the human-robot cooperation planner to an external disturbance would be to interpret the disturbance as a human input. This may result in the robotic system giving the lead to the human along an axis that the human did not intend to lead. However, this also has a benefit. One of the potential sources of external disturbances is the robotic system coming into contact with something unexpected. The robotic system giving leadership to the human along axes that correspond to the unexpected contact reduces the likelihood that the robotic system would further drive the arm into the unexpected object.

Moving forward there are additional areas of research to pursue. A number of values used in this experiment were determined from previous experiments and an initial pilot study. While these we useful for the purposes of this study, further research should examine these values. To additionally move the field closer to being able to operate in an unstructured environment, these values should be investigated for converting them from constant values to ones that are adapted to the environment, task, and person. Additionally, the system here used cartesian coordinates that are aligned both with the robotic system and with the task requirements. We feel that this could additionally be adapted to the task of the system. With an additional ability for the robot to identify what the likely external task is, the system could potential align the cartesian axes of the leader/follower DOF to a random task. Additional, the system potentially could identify different coordinate systems that might better align with different types of tasks.

REFERENCES

[1] H. I. Krebs *et al.*, "Rehabilitation robotics: Pilot trial of a spatial extension for MIT-Manus," *J. NeuroEng. Rehabil.*, vol. 1, no. 1, p. 5, 2004.

[2] C. J. Walsh, D. Paluska, K. Pasch, W. Grand, A. Valiente, and H. Herr, "Development of a lightweight, underactuated exoskeleton for load-carrying augmentation," in *Proc. IEEE Int. Conf. Robot. Autom. (ICRA)*, May 2006, pp. 3485–3491.

[3] J. Ward, A. Boehler, D. Shin, K. Hollander, and T. Sugar, "Control architectures for a powered ankle foot orthosis," *Int. J. Assist. Robot. Mech.*, vol. 9, no. 2, pp. 2–13, 2008.

[4] S. Y. Lee, K. Y. Lee, S. H. Lee, J. W. Kim, and C. S. Han, "Human-robot cooperation control for installing heavy construction materials," *Auto. Robots*, vol. 22, no. 3, pp. 305–319, 2007.

[5] S. Ikemoto, H. B. Amor, T. Minato, B. Jung, and H. Ishiguro, "Physical human-robot interaction: Mutual learning and adaptation," *IEEE Robot. Autom. Mag.*, vol. 19, no. 4, pp. 24–35, Dec. 2012.

[6] S. Calinon, F. Guenter, and A. Billard, "On learning, representing, and generalizing a task in a humanoid robot," *IEEE Trans. Syst., Man, Cybern. B, Cybern.*, vol. 37, no. 2, pp. 286–298, Apr. 2007.

[7] D. Kulić and Y. Nakamura, "Incremental learning of full body motion primitives," in *From Motor Learning to Interaction Learning in Robots*. Berlin, Germany: Springer, 2010, pp. 383–406.

[8] K. Kosuge, H. Yoshida, and T. Fukuda, "Dynamic control for robot-human collaboration," in *Proc. 2nd IEEE Int. Workshop Robot Human Commun.*, Nov. 1993, pp. 398–401.

[9] V. Duchaine and C. M. Gosselin, "General model of human-robot cooperation using a novel velocity based variable impedance control," in *Proc. 2nd Joint EuroHaptics Conf. Symp. Haptic Inter. Virtual Environ. Teleoper. Syst. (WHC)*, Mar. 2007, pp. 446–451.

[10] B. Corteville, E. Aertbeliën, H. Bruyninckx, J. De Schutter, and H. Van Brussel, "Human-inspired robot assistant for fast point-to-point movements," in *Proc. IEEE Int. Conf. Robot. Autom.*, Apr. 2007, pp. 3639–3644.

[11] A. Bussy, P. Gergondet, A. Kheddar, F. Keith, and A. Crosnier, "Proactive behavior of a humanoid robot in a haptic transportation task with a human partner," in *Proc. 21st IEEE Int. Symp. Robot Human Interact. Commun. (IEEE RO-MAN)* , Sep. 2012, pp. 962–967.

[12] T. Tsumugiwa, R. Yokogawa, and K. Hara, "Variable impedance control with virtual stiffness for human-robot cooperative task (human-robot cooperative peg-in-hole task)," in *Proc. IEEE/RSJ Int. Conf. Intell. Robots Syst.*, vol. 2. Aug. 2002, pp. 1075–1081.

[13] C. Passenberg, R. Groten, A. Peer, and M. Buss, "Towards real-time haptic assistance adaptation optimizing task performance and human effort," in *Proc. IEEE World Haptics Conf. (WHC)*, Jun. 2011, pp. 155–160.

[14] R. Groten, D. Feth, H. Goshy, A. Peer, D. A. Kenny, and M. Buss, "Experimental analysis of dominance in haptic collaboration," in *Proc. 18th IEEE Int. Symp. Robot Human Interact. Commun. (RO-MAN)*, Sep. 2009, pp. 723–729.

[15] C. E. Madan, A. Kucukyilmaz, T. M. Sezgin, and C. Basdogan, "Recognition of haptic interaction patterns in dyadic joint object manipulation," *IEEE Trans. Haptics*, vol. 8, no. 1, pp. 54–66, Jan. 2015.

[16] N. Stefanov, A. Peer, and M. Buss, "Role determination in human-human interaction," in *Proc. 3rd Joint EuroHaptics Conf. Symp. Haptic Interfaces Virtual Environ. Teleoper. Syst., World Haptics*, Mar. 2009, pp. 51–56.

[17] R. Groten, D. Feth, A. Peer, and M. Buss, "Shared decision making in a collaborative task with reciprocal haptic feedback—An efficiency-analysis," in *Proc. IEEE Int. Conf. Robot. Autom. (ICRA)*, May 2010, pp. 1834–1839.

[18] K. B. Reed and M. A. Peshkin, "Physical collaboration of human-human and human-robot teams," *IEEE Trans. Haptics*, vol. 1, no. 2, pp. 108–120, Jul. 2008.

[19] C. A. C. Parker and E. A. Croft, "Experimental investigation of human-robot cooperative carrying," in *Proc. IEEE/RSJ Int. Conf. Intell. Robots Syst.*, Sep. 2011, pp. 3361–3366.

[20] S. O. Oguz, A. Kucukyilmaz, T. M. Sezgin, and C. Basdogan, "Haptic negotiation and role exchange for collaboration in virtual environments," in *Proc. IEEE Haptics Symp.*, Mar. 2010, pp. 371–378.

[21] T. Wojtara *et al.*, "Human–robot collaboration in precise positioning of a three-dimensional object," *Automatica*, vol. 45, no. 2, pp. 333–342, 2009.

[22] M. Lawitzky, A. Mörtl, and S. Hirche, "Load sharing in human-robot cooperative manipulation," in *Proc. 19th Int. Symp. Robot Human Interact. Commun.*, Sep. 2010, pp. 185–191.

[23] P. Evrard and A. Kheddar, "Homotopy switching model for dyad haptic interaction in physical collaborative tasks," in *Proc. 3rd Joint EuroHaptics Conf. Symp. Haptic Interfaces Virtual Environ. Teleoper. Syst., World Haptics*, Mar. 2009, pp. 45–50.

[24] A. Kucukyilmaz, T. M. Sezgin, and C. Basdogan, "Intention recognition for dynamic role exchange in haptic collaboration," *IEEE Trans. Haptics*, vol. 6, no. 1, pp. 58–68, 1st Quart., 2013.

[25] Z. Wang, A. Peer, and M. Buss, "An HMM approach to realistic haptic human-robot interaction," in *Proc. 3rd Joint EuroHaptics Conf. Symp. Haptic Interfaces Virtual Environ. Teleoper. Syst., World Haptics*, Mar. 2009, pp. 374–379.

[26] A. De Santis, B. Siciliano, A. De Luca, and A. Bicchi, "An atlas of physical human–robot interaction," *Mech. Mach. Theory*, vol. 43, no. 3, pp. 253–270, 2008.

[27] N. Hogan, "Impedance control: An approach to manipulation: Part II—Implementation," *J. Dyn. Syst. Meas. Control*, vol. 107, no. 1, pp. 8–16, 1985.

[28] T. Flash and N. Hogan, "The coordination of arm movements: An experimentally confirmed mathematical model," *J. Neurosci.*, vol. 5, no. 7, pp. 1688–1703, Jul. 1985.

[29] B. Whitsell and P. Artemiadis, "On the role duality and switching in human-robot cooperation: An adaptive approach," in *Proc. IEEE Int. Conf. Robot. Autom. (ICRA)*, May 2015, pp. 3770–3775.

BRYAN WHITSELL (M'16) received the B.S. degree in mechanical engineering from the Rose-Hulman Institute of Technology, Terre Haute, IN, USA, and the M.S. degree in mechanical engineering from Arizona State University, Tempe, AZ, USA, in 2014, where he is currently pursuing the Ph.D. degree in mechanical engineering. He was a Mechanical Engineer and designed a wide variety of systems to enable testing of military equipment.

PANAGIOTIS ARTEMIADIS (SM'17) received the Diploma and Ph.D. degrees in mechanical engineering from the National Technical University of Athens, Athens, Greece, in 2003 and 2009, respectively. From 2009 to 2011, he was a Post-Doctoral Research Associate with the Newman Laboratory for Biomechanics and Human Rehabilitation, Mechanical Engineering Department, Massachusetts Institute of Technology, Boston, MA, USA. Since 2011, he has been with Arizona State University, Tempe, AZ, USA, where he is currently an Associate Professor with the Mechanical and Aerospace Engineering Department and the Director of the Human-Oriented Robotics and Control Laboratory. His research interests lie in the areas of robotics, control systems, system identification, brain–machine interfaces, rehabilitation robotics, neuro-robotics, orthotics, human motor control, mechatronics, and human–robot interaction.